PORE GEOMETRY AND ROCK PROPERTIES

Peter R. Whattler, Enterprise Oil plc

Paul B. Basan, Applied Reservoir Technology Ltd

Brian P. Moss, Moss Petrophysics

ABSTRACT

This article summarises the early results of a research project carried out over the past 4 years. The principle objective of the project, was to compare special core analysis measurements with parameters derived from the processing of back scattered electron images. The data base consists of 82 samples from 9 wells. Each sample has Ø, k_{air}, FRF and pore measurements acquired from 1066 image fields, (13/sample).

We found the linear equation using pore area, (image porosity), predicts permeability with a Standard Error of the Mean, (σ), of 0.284 $\log_{10}$ permeability units. Using a pore length squared, in addition to pore area, predicts permeability having σ = 0.266 $\log_{10}$ permeability units. For reference, core analysis porosity predicts permeability having σ = 0.637 $\log_{10}$ permeability units.

Following success with the prediction of permeability, the research focused on another simple flow-related property, Formation Resistivity Factor. It was found that the reciprocal of image porosity produced an acceptable estimator for a large proportion of the data set. It has been concluded therefore, that image porosity is probably a measure of the samples effective porosity rather than the total porosity.

The conclusion, therefore, is that the analysis of back scattered electron images produces both a diagnostic tool for evaluating differences in the rock properties from a reservoir sequence, and a method to calculate rock properties in the absence of more traditional data.

INTRODUCTION

A research project was conducted over the period 1990 to 1994. The project involved generating a truly quantitative petrographic and petrophysical data base. The petrographic data was generated using an automated image analysis programme. These data are then used to investigate the links between pore geometry and various Special Core Analysis

measurements. This paper presents some initial findings regarding the influence of pore geometry, as defined using image analysis, on transport properties in a sandstone reservoir. The results that are presented within this paper are largely empirical. Yet it must be noted that throughout this study, the work of Perez-Rosales[10,11] Katz and Thompson[7,8] and latterly Herrick and Kennedy[6], was at the forefront of our thinking.

Background and objectives of the research

In the search to find ways of quantifying the amounts of hydrocarbon in the ground or the ease with which it will flow there are ever increasing numbers of empirical relationships that are employed. In the course of such work it has long been recognised that there is strong evidence for there being a relationship between the texture or nature of the rock fabric and the measured parameters. Many authors[1,3,4,5,9,12,13,14&15] have attempted to quantify this relationship either by looking at the mineral grains or else the pores themselves. However the lack of an objective and consistently reproducible means of describing the observed rock fabric has caused the pursuit of the relationship to remain unresolved.

The Image Analysis technique is believed to overcome the problems of subjectivity offering new and different measurements to quantify rocks. Image analysis is not new, many authors have used image analysis to examine rocks. The published work can largely be sub-divided into papers that seem to be concerned with either reproducing the measured core porosity, or else constructing volume elements from the surface openings. Thus, while previous work demonstrates results, it does not explain the links between image analysis and core analysis for determining different attributes of pore geometry. Neither do these publications provide much guidance on how to apply pore geometry as a diagnostic nor predictive tool. Part of the overall research objective, therefore, was to establish the connection between core and image analysis data and to determine the link between pore geometry and familiar parameters like porosity, permeability and formation factor.

Samples and data base

The sample materials used in this study are the end trims from a mixture of routine and special core analysis plugs. In total 82 different samples from nine different North Sea wells, have been utilised in the course of this study. All these plugs are from rocks of Tertiary age which were deposited in a submarine fan environment as a result of density currents. The sediment contains a variety of mineral species indicative of a predominantly metamorphic source. All the lithofacies therefore contain some amount of deformable particles. The plugs themselves have been subjected to a broad spectrum of measurements, although not every plug has necessarily had all measurements made on it. All of these measurements have been collated together to form the database for this project.

Throughout this paper it will be observed that well E is consistently an outlier to the main relationship and does not conform. A full discussion of the work that has been undertaken to investigate this well is beyond the scope of this paper. Suffice to say that it is believed that the rather simplistic data reduction methods that have been employed have masked a real fabric variation. As a consequence of this, all statistical analysis has been conducted ignoring this well. For completeness and to illustrate the problems of working with real data all plots include data from well E, which are coded with the symbol '*'.

Description of the Image Analysis Technique

Whereas there are recommended practices for the experiments that generate core analysis measurements, the image analysis technique that has been employed in this work is not defined by recommended practice. There are many choices for the user of image analysis to make before quantified image parameters can be derived. A full detailed explanation of these choices and the ones selected in this work, is beyond the scope of this paper.

IMAGE ANALYSIS AND ITS RELATIONSHIP TO POROSITY

If one considers regular packs of spherical objects, then the porosity of such systems is constant, irrespective of the size of the spheres themselves. What varies as the grain size changes are the number of spheres, the surface area and the size of the interstices. However natural rocks are neither regularly packed nor uni-modal in grain size. Hence observation of real rocks consistently indicate that porosity will reduce as the grain size reduces. In view of this, there was a high expectation that a strong relationship between core porosity and image analysis parameters would have been observed.

The openings observed on a sample surface represent pore area rather than pore volume and this area represents just one random part of the total pore system. The basis for attempting to equate image porosity with core porosity arises from the Delesse[2] principle which proposes that area gives an unbiased estimate of volume for pore systems that are isotropic and homogeneous. Therefore

$$\text{Porosity from Image Analysis} = \frac{\text{Area of Pore Space}}{\text{Total Area}} \qquad ①$$

The image analysis technique that has been employed is specifically designed to examine the pore space. Hence a simple ratio of the number of pixels having resin grey scale divided by the total number of pixels in the field of view should equate to image analysis porosity.

Every plug within the database has had its porosity measured by gas expansion and in a number of cases this porosity measurement has been repeated by different laboratories. A comparison of the image analysis porosity to that measured by gas expansion is depicted in Figure 1. This plot indicates that the image analysis porosity is underestimating the porosity

measured by gas expansion. Furthermore there appears to be little consistency between the two measurements.

A possible reason for the discrepancy may be that a two dimensional slice does not truly represent the complete three dimensional pore system. However, the fact that other authors have predicted pore volume satisfactorily from images suggests that other factors may be at play here. That the image analysis porosity is consistently less than the gas expansion porosity and not randomly scattered about the equality line suggests that the two experiments are not sensing the same phenomena. In the image analysis experiment which has been conducted, only two levels of magnification: x 30 and x 150 are used. These magnifications were deliberately chosen to focus on the largest pores. It is recognised that micro pores will be overlooked. Figure 1 suggests that between 10 to 15 porosity units, (40-50% of the gas expansion pore volume), is not detected by image analysis using our method. This difference between conventional core porosity and image porosity is often a concern because of the implications for reserves calculations.

Part of the difference is explained by the difference in techniques. Conventional core analysis employs a thoroughly cleaned and dried sample that is measured by expanding helium through the core plug. The measurement is typically considered the maximum measurement of porosity because gas molecules fill all the connected pore. In the reservoir this volume contains both irreducible water, either held in small voids or bound to the surface of larger voids, plus movable fluids. Unfortunately no one knows the true effective volume at reservoir conditions that is occupied by mobile fluids.

Image analysis measures a resin filled area on a core plug surface. The limits of the measurement are largely controlled by the ability of the system to distinguish grey-levels of the filling epoxy and any other phase contained in the image, and by limitations on setting a minimum stack of pixels to actually define an open void. The image analyser which has been used for this work is set for a minimum equivalent diameter of about 3μm. A micro-pore, by comparison, is conventionally defined as having a diameter of less that 1μm. The 2μm difference undoubtedly accounts for a large number of individual voids, and as yet an unknown quantity of porosity.

$$\emptyset_{gex} = \emptyset_{IA} + \emptyset_{(3\text{-}1)} + \emptyset_{\mu} \qquad (2)$$

Where:

- $\emptyset_{gex}$ Conventional routine core analysis gas expansion porosity
- $\emptyset_{IA}$ Image Analysis porosity estimate
- $\emptyset_{(3\text{-}1)}$ Porosity contributed by pores between 3 and 1 microns in diameter
- $\emptyset_{\mu}$ Micro porosity (Porosity contributed by pores less than 1 microns in diameter)

The fraction of porosity in the $\emptyset_{(3\text{-}1)}$ size range remains un-quantified and its contribution to the rock petrophysical properties remains unresolved.

It is our belief that the procedures used provide a reliable, consistent and repeatable method for estimating a pore volume. However the actual values derived from this image analysis technique are different. It is our hypothesis that image analysis porosity is more likely to represent or reflect the "effective" porosity, or the flowing porosity, of Perez-Rosales[11], rather than the total porosity that the industry traditionally recognises as a definitive value.

IMAGE ANALYSIS AND ITS RELATIONSHIP TO PERMEABILITY

Following similar logic to that employed when considering porosity, permeability is grain size dependant. The ability of a system to conduct fluid is dependant upon the size of the path ways available for flow. Since image analysis actually makes measurement upon the actual pore system it was felt that a good correlation should be expected.

Permeability is a dynamic property of the rock and porosity a static property, a comparison of these two properties is commonly used by geo-scientists to characterise rock fabrics. A crossplot of these two parameters, Figure 2, for the data used in this study, is presented. Normally for natural rocks, observation of these two parameters reveals acceptable correlation, although often with the large spread of permeability and rather limited range of porosity, as seen in Figure 2. In consequence core porosity represents a poor predictor of permeability. This is particularly so in the case of this data set, as illustrated by linear regression statistics[♦] of $R^2 = 0.273$ and $\sigma = 0.637$.

Permeability, the conductivity of the rock, should be dominated by the biggest pathways through the rock. If this is so, then a porosity measure that sees only the larger pores may well represent a good permeability predictor. A crossplot of porosity derived from image analysis versus core air permeability, Figure 3, shows a much stronger linear relationship. This plot clearly indicates that simple image porosity, while it may not describe total porosity, it may indeed provide a robust means of predicting permeability. Linear regression was performed which generated equation ③

$$Log10(\text{Permeability}) = 0.244 + (16.620 \times (\text{Image Porosity}) \qquad ③$$

The regression generated values of $R^2 = 0.855$ and $\sigma = 0.284$. The values predicted by this equation are plotted against the measured values in Figure 4. This seems to be a fairly effective yet simple predictor that can be explained as follows. Image porosity is not total porosity and this difference has been ascribed to the fact that our image analysis experiment

♦ Reminder -- All regression is performed excluding well E

sees preferentially the larger pores. It is therefore inferred that the transport property of the rock is described, to a first order, by the largest pores, which make up the greater part of the cross sectional area available for flow.

Looking at the form of the Darcy relationship, permeability has dimensions of length squared. Image porosity is a dimensionless quantity and, as such, equation ③ does not have the correct dimensions. Studies addressed devising and testing of equations that did have the correct dimensions, with the result that equation ④ was derived.

$$Log10(\text{Perm}) = \text{const.}1 + (\text{const.}2 \times \text{length}^2) + (\text{const.}3 \times \text{Image Porosity}) \quad ④$$

The image analysis we use generates a total of 64 chord lengths for each pore. These are then manipulated to generate the various diameters and radii that describe the pores. In equation ④ the specific choice of which diameter or radii to use to represent the length term, is somewhat user dependent. In some data sets the appropriate choice eliminates the need for the pre multiplier but not in this data set. In equation ⑤ the length term is represented by the average maximum chord length. Linear regression generated the following equation thus:

$$Log10(\text{Perm}) = 0.280368 + (0.000309 \times \text{length}^2) + (14.03538 \times \text{Image Porosity}) \quad ⑤$$

The regression computed values of $R^2 = 0.875$ and $\sigma = 0.266$. The estimates predicted by this equation are plotted against the measured values in Figure 5. The difference between Figure 4 and Figure 5 is not marked but in terms of t-test statistics, the length squared term is making a real and significant contribution. The computed t-test statistic of t=3.38 is significant at well below 1%. This is evidenced by the data being somewhat tighter clustered around the equality line.

The use of average maximum chord length in equation ⑤ was questioned as perhaps being an inappropriate choice since it reflects the largest dimension of the pore. The breadth parameter on the other hand reflects the minimum dimension of the pore. Permeability is commonly held to be controlled by the smallest dimensions. Thus it was suggested that breadth could be more effective. Regression using breadth resulted in equation ⑤a:

$$Log10(\text{Perm}) = 0.295949 + (0.001004 \times \text{breadth}^2) + (13.86069 \times \text{Image Porosity}) \quad ⑤a$$

This regression generated identical values of R^2 and σ to those obtained when using length. Only the t-test parameter changed slightly, t=3.40,. Estimates predicted by this equation are not presented since the actual variations are minor. The plot is very similar to Figure 5 with occasional points moved.

From the above observations the conclusion is drawn that image porosity represents the primary control on permeability. Furthermore it can also be concluded that only a proportion, generally less than 50% of the total pore system, is significant in the flow of gas molecules. The addition of a length descriptor of the pore system, improves the prediction but the choice of length parameter appears to be somewhat arbitrary.

IMAGE ANALYSIS AND ITS RELATIONSHIP TO FORMATION FACTOR

Formation Resistivity Factor, FRF, is a measure of relative transport capacity of the rock to electrically charged species. An electron, or an ion in solution, is smaller than a gas molecule and certainly more likely to be reactive with the matrix. Despite this it is a dynamic, or conductivity property of the rock and was expected, to a first approximation, to be controlled by similar phenomena as permeability.

Archie determined that electrical resistivity has a simple relationship to the pore geometry expressed by the equation: $\text{Formation Resistivity Factor} = \frac{a}{\Phi^m}$. In this equation the exponent "m" modifies porosity to characterise the effective current volume. A conventional crossplot of the formation resistivity factor versus core porosity, Figure 6, illustrates the data used in this study. From this plot it will be observed that this data set is relatively well behaved and tightly clustered. The gradient of the line from any data point to the water point is equal to "*m*" and is commonly called the cementation exponent. Following usual log analysis practice, the average value of these individual "*m*" values was found to be 1.78.

Since the image porosity proved so effective to describe the permeability, the logical first approach was simply to replace core porosity with image porosity in the Archie equation. Figure 7 shows a Crossplot of image porosity Vs formation resistivity factor. This plot illustrates a greater degree of scatter suggesting that the relationship to image parameters is perhaps not as straight forward as for permeability. Individual "*m*" values were calculated for each point and averaging these values equation ⑥ is derived.

$$FRF = \frac{1}{\left(\Phi_{\text{image}}\right)^{1.17}} \qquad ⑥$$

The exponent in equation ⑥ is close to one. This implies that FRF is tending toward being proportional to the reciprocal of the image porosity. A plot of FRF versus the reciprocal of the image porosity, Figure 8, shows this relationship. Inspection of this plot reveals the presence of two trends. The first, (Trend A), is parallel to, but offset from, the unity line. The other, (Trend B), is shallower having FRF increasing at a slower rate than the reciprocal of the image porosity. Trend B is largely constituted by the data from well E. For this reason it is considered a high probability, though not yet substantiated, that this could be an artefact of the data reduction that we have employed. Trend A supports the hypothesis that FRF is proportional to the inverse of image porosity. Assuming a reciprocal relationship and applying it to the Trend A data set, causes an offset of 4.3 to be computed. Hence a predictor for FRF could be derived from equation ⑦

$$FRF = 4.3 + \frac{1}{\Phi_{\text{image}}} \qquad ⑦$$

The Trend A data set constitutes at least 80% of the total data. Using equation ⑦ to predict FRF, will generate reasonable estimates that have the same amount of scatter as that evidenced in Figure 8. However this achievement is recognised to be limited without a definitive explanation for the Trend B data.

An alternative approach that was attempted, was to retain core porosity in the Archie equation and to try to recreate the effect of the cementation factor using parameters from image analysis. It was found that the ratio $\left(\frac{\text{Pore Length}}{\text{Pore Breadth}}\right)$, has values similar to the cementation exponent. Initially it was thought this result suggested that the cementation exponent, "*m*", is dependent upon the aspect of the pore system. However a crossplot of "m" versus the length over breadth ratio showed no clear relationship. In practice the two numbers have very similar ranges and value of central tendency. The fact that this parameter had provided a satisfactory predictor, when used to modify core porosity, is viewed for the moment to be coincidental.

DISCUSSION

We have demonstrated that predictors of flow properties can be generated by analysing back scattered electron microscope images of the rock. Analysis of these images quantifies the pore system and thereby allows the possibility of examining the pore geometry controls on rock properties. The challenge of reducing approximately two and a half million pixels of information in order to compare it to a single core analysis measurement should not be underestimated. Many assumptions are made in this reduction, any one of which will ultimately effect the end result. Additionally the measurement of flow properties is well renowned for its sources of error. In consequence it is recognised that there is a huge amount of data analysis still to be conducted.

Despite this, the fact remains that images capture a significant fraction of the pore volume controlling to the rock flow parameters, permeability and FRF. It is recognised that the FRF equation presented, does not describe all of the data set. However these permeability and FRF relationships have been tested on other data sets with similar results. These additional data sets contain samples ranging from Tertiary to Carboniferous in age and both having tight and permeable rocks. In consequence we believe that the simple image porosity parameter is probably equivalent to the 'effective' or 'flowing' porosity of the literature. This belief is further supported by the strong relationship with the free fluid index of nuclear magnetic resonance[16].

CONCLUSIONS

At the magnifications that have been used in this study, the porosity derived from image analysis is always smaller than porosity from routine core analysis. Yet no obvious correlation is observed between these two measures. Therefore the image analysis which has been performed does not represent a means of predicting total porosity.

What image porosity does provide is a good basis for predicting a rocks flow properties. Permeability is well predicted by image porosity and slightly further improved by the addition of a pore size dimension. Prediction of Formation Resistivity Factor is less robust, but is adequately predicted for the majority of these data. It is therefore concluded that image porosity is a simple and reliable measurement that is equivalent to the effective or flowing porosity of the literature.

References

1 Clelland, W. D., et al., 1993. Quantitative analysis of pore structure and its effect on reservoir behaviour: Upper Jurassic Ribble Member sandstones, Fulmar Field, UK North Sea. *In:* Ashton, M. (ed.), Advances in Reservoir Geology, Geol. Soc. Spec. Publ. 69:57-79.

2 Delesse, M.A., 1847. Procédé mécanique pour déterminer la composition des roches. C.R. Acad. Sci., Vol.25, 544.

3 Dilks, A and Graham, S. C., 1985. Quantitative mineralogical characterisation of sandstones by back scattered electron image analysis. Jour. Sed. Pet., 55:347-355.

4 Ehrlich, R., et al., 1984. Petrographic image analysis, I. Analysis of reservoir pore complexes. Jour. Sed. Pet., 54:1365-1378.

5 Ehrlich, R., et al., 1991a Petrography and reservoir physics I: Objective classification of reservoir porosity. Am. Assoc. Petrol. Geol. Bull., 75:1547-1562.

6 Herrick, D. C. and Kennedy, W. D.,1993. Electrical Efficiency: A pore geometric model for the electrical properties of rocks. SPWLA 34th Ann Log Symp, Paper HH.

7 Katz, A. and Thompson, A., 1986. Quantitative prediction of permeability in porous rock. Phys. Rev. Bul, 8179-8181

8 Katz, A. and Thompson, A., 1987. Prediction of rock electrical conductivity from mercury injection measurements. Jour. Geop. Res., Vol. 92, 599-607.

9 Nadeau, P.H. and Hurst, A. 1991. Application of backscattered electron microscopy to the quantification of clay mineral micro porosity in sandstones. Jour. Sed. Pet., 61:921-925.

10 Perez-Rozales, C., 1976. Generalisation of the Maxwell Equation for Formation Resistivity Equation. JPT. 819-824.

11 Perez-Rosales, C., 1982. On the relationship between formation resistivity factor and porosity. SPE. Jour. 531-536.

12 Riable, C., et al., 1989. Static pore structure analysis of reservoir rocks. US Dept. Energy Enhanced Oil Recovery Report, 76-79.

13 Ruzyla, K., 1986. Characterisation of pore space by quantitative image analysis. SPE Form. Eval., 1:389-398.

14 Ruzyla, K., 1988. Limitations and pitfalls of using quantitative image analysis for reservoir assessment (Abs). Am. Assoc. Petrol. Geol. Bull., 72:243.

15 Yuan, Li-Ping, 1990. Pore image characterisation and its relationship to permeability. SCA paper 90002, Soc. Core Analysts Conf., 1-18.

16 Basan, P., 1995. Pore size data in petrophysics: A perspective on pore geometry. In Prep.

Fig 1. Core Porosity Vs Image Porosity

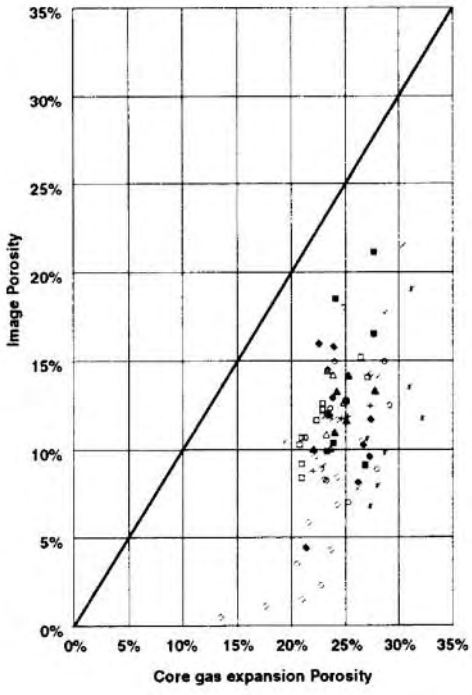

Fig 2. Core Porosity Vs Permeability

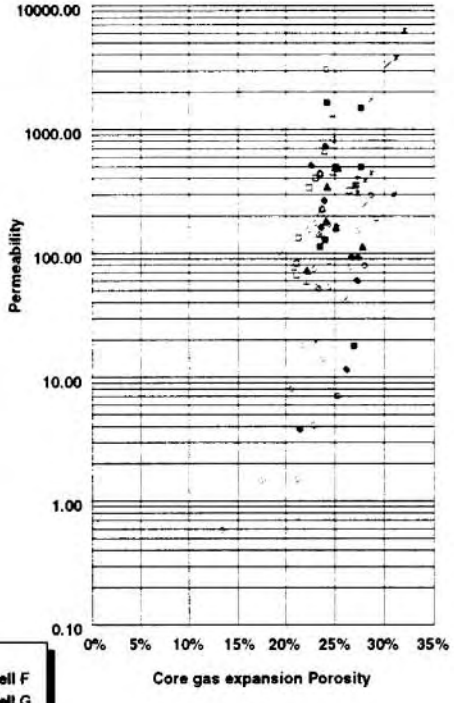

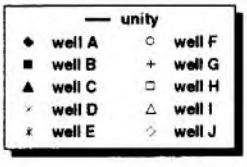

Fig 3. Image Porosity Vs Permeability

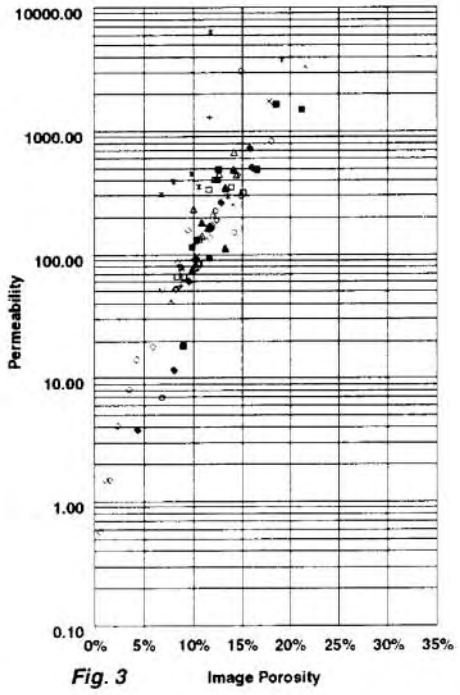

Fig. 3

Fig 4. Permeability predicted by Eq 3 Vs Measured Permeability

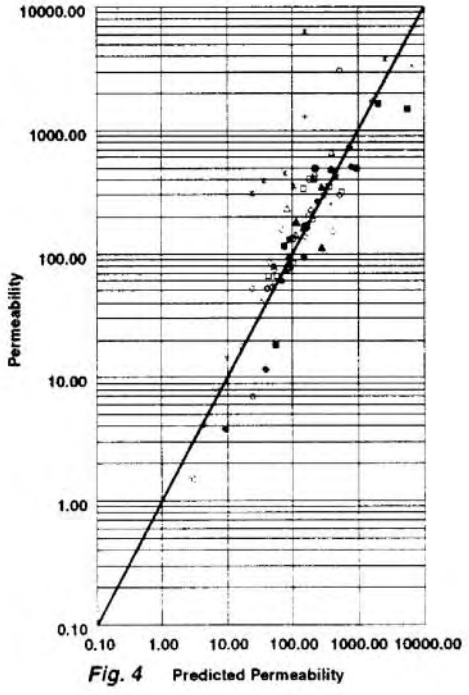

Fig. 4

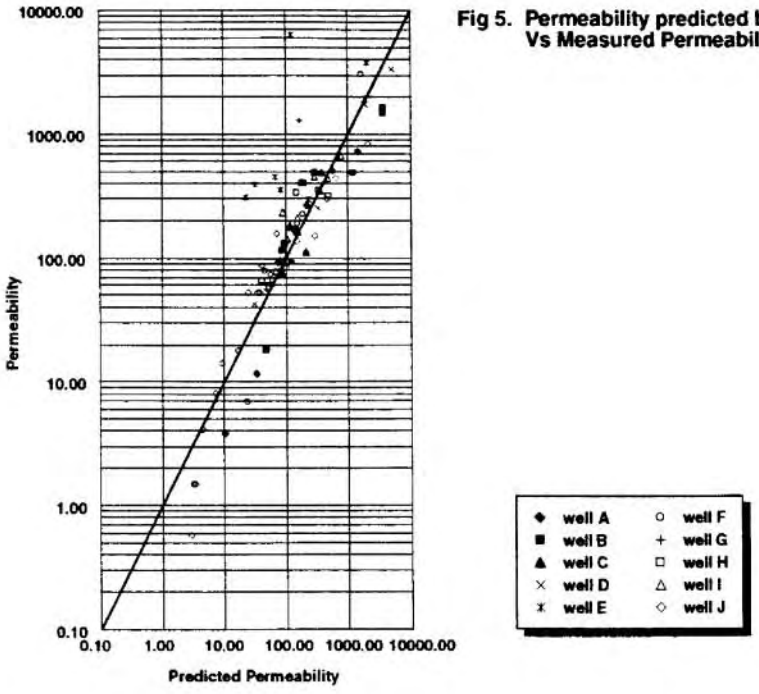

Fig 5. Permeability predicted by Eq 4 Vs Measured Permeability

Fig 6. Image Analysis Porosity Vs Formation Resistivity Factor

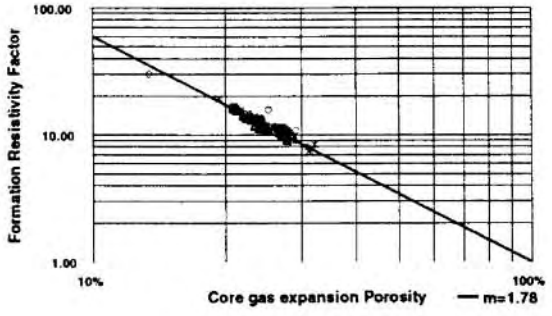

Fig 7. Core Porosity Vs Formation Resistivity Factor

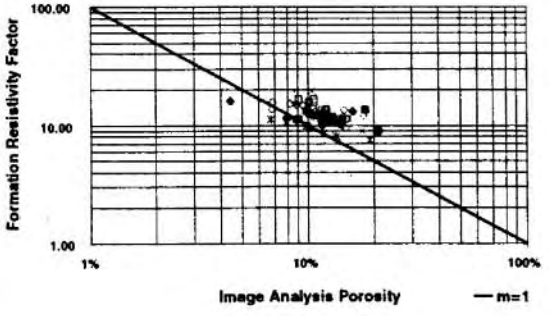

Fig 8. Reciprocal of Analysis Porosity Vs Formation Resistivity Factor

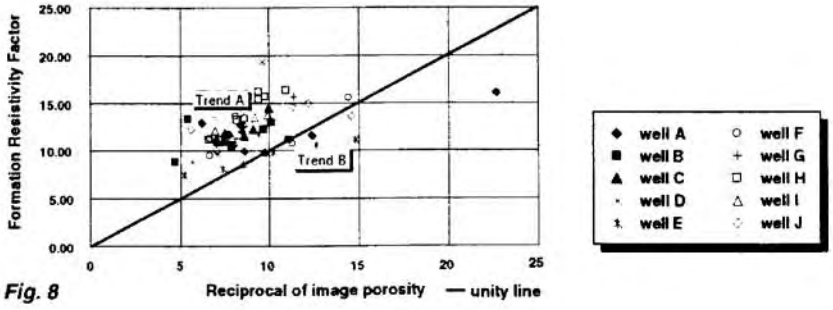

Fig. 8